

# Evaluating expression patterns of multiple inhibitory and stimulatory receptors on natural killer cells using flow cytometry

Using the BD LSRFortessa™ X-20 cell analyzer and BD Horizon Brilliant™ Ultraviolet reagents enables detection of up to 18 markers simultaneously and offers flexibility in panel design

## Features

- Resolve natural killer (NK) cell heterogeneity
- Simultaneously assess stimulatory and inhibitory receptor expression on NK cells using an 18-color flow cytometry panel
- Reveal donor-specific differences in NK cell diversity using high-dimensional data analysis tools

Natural killer cells are an important part of the innate immune system and constitute a frontline defense in the killing of virally infected and malignant cells through the secretion of cytotoxic granules containing granzymes, perforin and granulysin. Activated NK cells also secrete a milieu of cytokines that regulate the function of other cells that play roles in innate and adaptive immune responses, including dendritic cells, macrophages, neutrophils and antigen-specific T and B cells.

NK cell function is tightly regulated by stimulatory and inhibitory receptors that recognize cellular stress ligands as well as human leucocyte antigen class I (HLA class I). Inhibitory signals are particularly important for the maintenance of self-tolerance in a class-I-dependent manner while stimulatory signals drive NK-cell effector functions.

A series of stimulatory and inhibitory receptors can be expressed in a stochastic, variegated and overlapping way on the surface of NK cells, with estimates of greater than 30,000 NK cell phenotypes in a given individual. NK cells also display extensive phenotypic diversity among individuals, with inhibitory receptor expression being largely determined by genetics and stimulatory receptor expression being heavily driven by environmental factors and/or stochastic influences.



In this data sheet, we describe a flow-cytometry-based immunophenotyping assay to define the major subsets of human NK cells and to further characterize the expression of key stimulatory and inhibitory receptors. The expression of key stimulatory or inhibitory receptors was first studied separately using two 12-color flow cytometry panels on the BD LSRFortessa™ cell analyzer. This enabled the simultaneous assessment of a backbone panel of six NK cell lineage markers in combination with either six stimulatory or inhibitory markers. We then combined these markers, creating an 18-color panel to simultaneously assess all markers in one tube and research further into the NK cell heterogeneity across five donors. Using the 355-nm ultraviolet (UV) option on the BD LSRFortessa™ X-20 cell analyzer and the associated BD Horizon Brilliant™ Ultraviolet (BUV) reagents allowed us to spread these 18 markers across an additional laser line and more spectral space which can simplify panel design due to more fluorochrome choice and less dye overlap.

To investigate multiple NK-cell phenotypes in a single individual, we used a modular panel-design strategy. This approach enabled us to characterize the major NK-cell subsets using a 6-color backbone panel and to assess the expression of either stimulatory or inhibitory receptors by using two alternative 6-color drop-in panels (Table 1). This modular panel-design strategy provides researchers the flexibility to swap the markers in the drop-in panel with their preferred markers.

Table 1. Modular 12-color panel with a 6-color backbone to identify major NK subsets and 6-color drop-in panels to assess stimulatory or inhibitory receptor expression on NK cells

6-Color Backbone Panel			6-Color Drop-In: Stimulatory Panel		6-Color Drop-In: Inhibitory Panel			
	Specificity	Fluorochrome	Specificity	Fluorochrome	Specificity	Fluorochrome		
Major NK Subsets	CD94	BV480	Stimulatory Receptors	CD314 (NKG2D)	BV421	Inhibitory Receptors	CD158f (KIR2DL5)	BV421
	CD16	BV786		CD159c (NKG2C)	BV605		CD158b (KIR2DL2/3)	BV605
	CD57	FITC		CD337 (Nkp30)	BV650		TIGIT	BV650
	CD56	PE-Cy™ 7		CD226 (DNAM-1)	BV711		CD159a (NKG2A)	BV711
	CD27	APC-R700		CD160	PE		CD158e1 (NKB1/KIR3DL1)	PE
	CD3	APC-H7		CD244 (2B4)	APC		CD158a (KIR2DL1)	APC

The 6-color backbone panel enabled the identification of developmentally and functionally distinct NK-cell subsets, based on the analysis of CD56 and CD16 expression profiles. CD56<sup>bright</sup>CD16<sup>-</sup> cells represent a small subset of immature, circulating NK cells that are potent cytokine producers but have low cytotoxic capacity before activation. CD56<sup>dim</sup>CD16<sup>+</sup> cells include terminally differentiated NK cells that exert cytotoxic functions and have limited ability to produce cytokines (Figure 1A).

CD56<sup>bright</sup> cells are known to undergo a continuum of differentiation that ends with the CD56<sup>dim</sup> phenotype. Analysis of CD94 expression helped to identify developmental intermediaries, such as CD94<sup>high</sup>CD56<sup>bright</sup>, CD94<sup>high</sup>CD56<sup>dim</sup> and CD94<sup>low</sup>CD56<sup>dim</sup>, the latter being the most cytotoxic subset (Figure 1B). Maturation of NK cells could also be monitored by analysis of the loss of CD27 and gain of CD57 on the surface of CD56<sup>dim</sup>CD16<sup>+</sup> cells, as compared to CD56<sup>bright</sup>CD16<sup>-</sup> cells (Figure 1C).

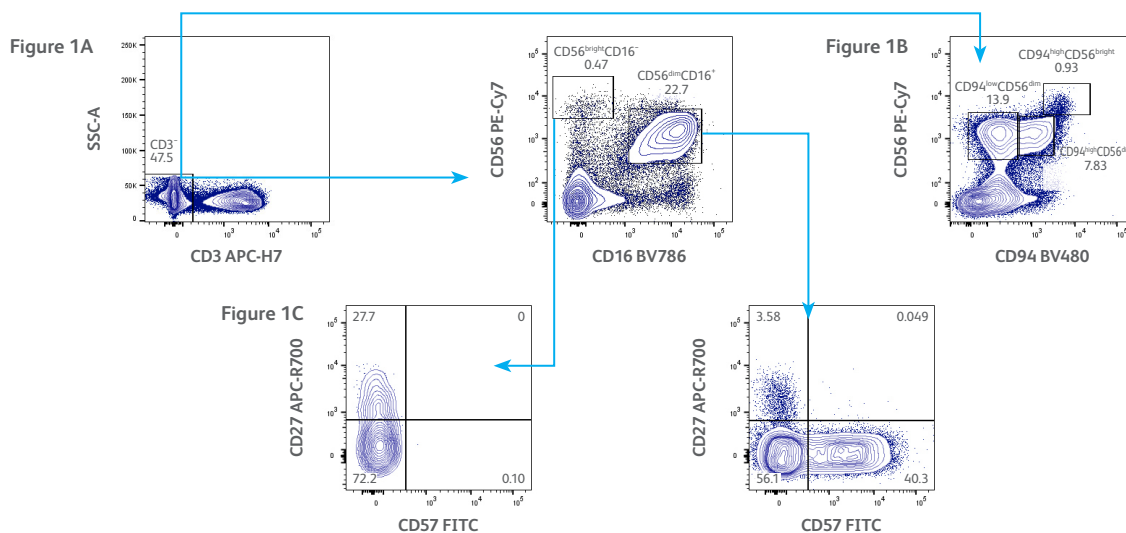
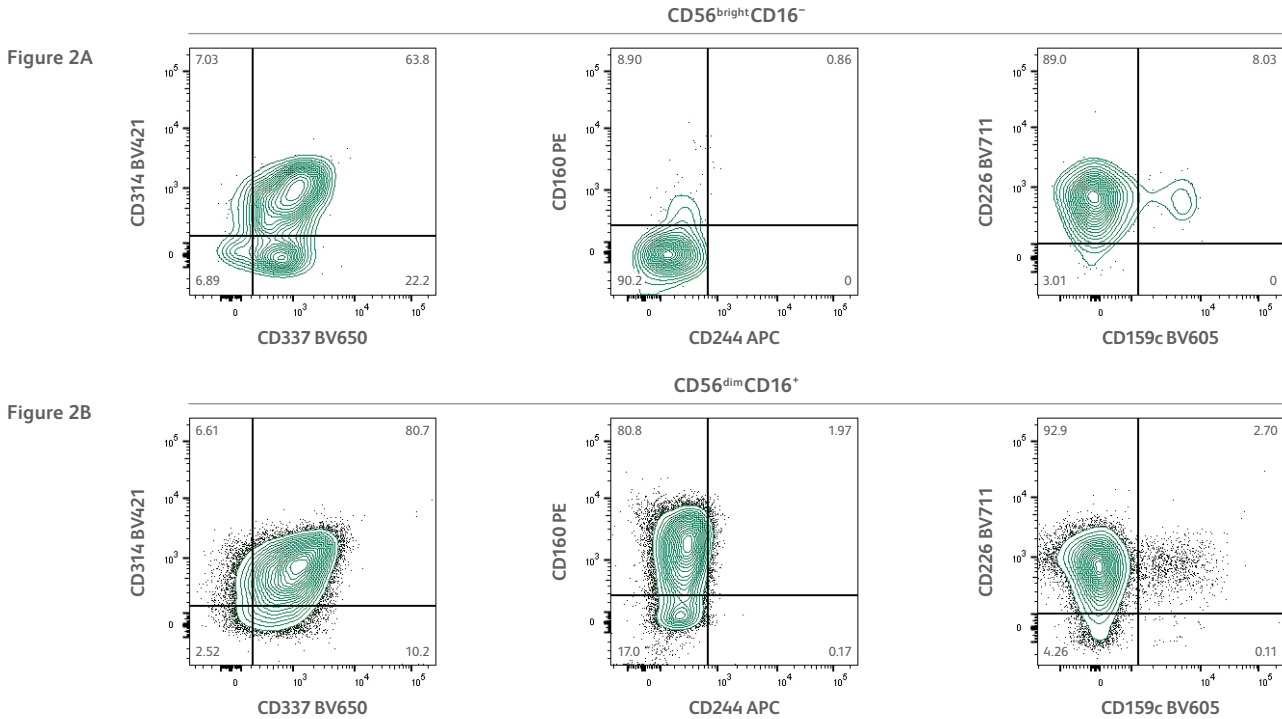


Figure 1. Gating strategy for analysis of the major NK subsets

Fresh blood cells from a healthy donor (Donor 1) were stained with the antibody-fluorochrome conjugates listed in Table 1. Whole blood was stained with the panel along with BD Horizon™ Brilliant Stain Buffer Plus for 30 minutes in the dark. Red blood cells were lysed for 15 minutes using the BD FACS™ Lysing Solution. Cells were washed twice using the BD Pharmingen™ Stain Buffer (FBS). Sample acquisition was completed on the BD LSRFortessa flow cytometer with a violet/blue/yellow-green/red laser configuration. A. Major NK-cell subsets were defined within the CD3<sup>+</sup> lymphocytes as CD56<sup>bright</sup>CD16<sup>-</sup> or CD56<sup>dim</sup>CD16<sup>+</sup> cells. B. CD94 expression identified developmental intermediaries of NK cells (CD94<sup>high</sup>CD56<sup>bright</sup>, CD94<sup>high</sup>CD56<sup>dim</sup> and CD94<sup>low</sup>CD56<sup>dim</sup>). C. NK cell maturation can be further assessed by analyzing the gain of CD57 expression and loss of CD27 expression on CD56<sup>dim</sup>CD16<sup>+</sup> cells, as compared to CD56<sup>bright</sup>CD16<sup>-</sup> cells. Population statistics are indicated for each gate in the respective contour plots.

The CD94 receptor can associate with various NKG2 family receptors, such as CD159c (NKG2C) and CD159a (NKG2A) in the drop-in panels, to form a heterodimer complex that recognizes nonclassical MHC class I molecules. Depending on the NKG2 family member, this complex can stimulate or inhibit cytotoxic activity of NK cells. The 6-color drop-in stimulatory panel enabled the analysis of two NKG2 family members, CD159c (NKG2C) and CD314 (NKG2D), in addition to CD337, CD226, CD160 and CD244 (Figure 2). The inhibitory panel contained an NKG2 family member, CD159a (NKG2A), in addition to TIGIT and killer immunoglobulin-like receptor (KIR) family members; CD158a, CD158b, CD158e1 and CD158f (Figure 3). Stimulatory and inhibitory receptors showed differential patterns of expression in CD56<sup>bright</sup>CD16<sup>-</sup> cells compared to CD56<sup>dim</sup>CD16<sup>+</sup> cells, such as higher levels of expression for stimulatory receptor CD160 and higher levels of inhibitory receptors TIGIT and KIR family members in the CD56<sup>dim</sup>CD16<sup>+</sup> population.



**Figure 2. Evaluation of stimulatory marker expression on the major NK subsets**

Major NK-cell subsets shown in Figure 1 (CD56<sup>bright</sup>CD16<sup>-</sup> and CD56<sup>dim</sup>CD16<sup>+</sup>) were assessed for expression of stimulatory markers CD337, CD244, CD226 and CD160 in addition to two members of NKG2 receptor family, CD159c (NKG2C) and CD314 (NKG2D), in the contour plots. **A.** Contour plots for the CD56<sup>bright</sup>CD16<sup>-</sup> cells. **B.** Contour plots for the CD56<sup>dim</sup>CD16<sup>+</sup> cells. Population statistics are indicated for each quadrant gate in the respective contour plots.

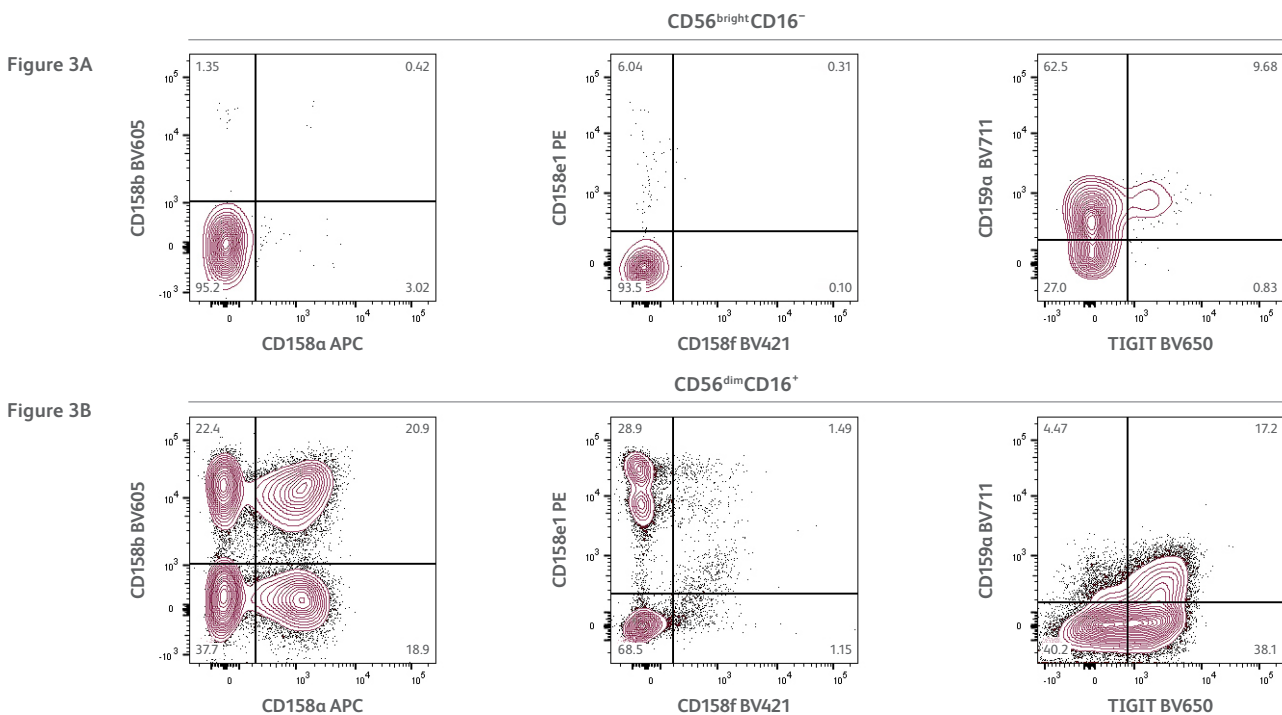


**Figure 3. Evaluation of inhibitory marker expression on the major NK subsets**

Major NK-cell subsets shown in Figure 1 (CD56<sup>bright</sup>CD16<sup>-</sup> and CD56<sup>dim</sup>CD16<sup>+</sup>) were assessed for expression of inhibitory markers CD158a, CD158b, CD158e1, CD158f, TIGIT and an NKG2 receptor family member CD159a (NKG2A) in the contour plots. **A.** Contour plots for the CD56<sup>bright</sup>CD16<sup>-</sup> cells. **B.** Contour plots for the CD56<sup>dim</sup>CD16<sup>+</sup> cells. Population statistics are indicated for each quadrant gate in the respective contour plots.

As mentioned, NK cells are highly heterogeneous; some individuals express a set of stimulatory and inhibitory receptors while others do not. NK cell function is controlled by combinatorially expressed stimulatory and inhibitory receptors, thus making NK-cell diversity and function closely linked. For simultaneous assessment of the combinatorial expression of stimulatory and inhibitory markers, we combined all the markers in a single 18-color panel (Table 2). This simplified the analysis of the multiple phenotypes of NK cells across different donors and provided a more comprehensive understanding of NK-cell diversity. In addition to CD94, CD57 and CD27, the surface expression of all the stimulatory and inhibitory markers was examined across five different donors revealing the differences in the expression of markers such as CD337, CD159a, CD158a and TIGIT (Figure 4).

Table 2. An 18-color panel for the analysis of 12 distinct stimulatory and inhibitory markers on subsets of human NK cells

Major NK Subsets	Specificity	Fluorochrome	Stimulatory Receptors	Specificity	Fluorochrome	Inhibitory Receptors	Specificity	Fluorochrome
	CD3	BUV563		CD226 (DNAM-1)	BV711		CD158b (KIR2DL2/3)	BUV395
	CD56	BUV737		CD159c (NKG2C)	BV786		CD158e1 (NKB1/KIR3DL1)	BUV805
	CD94	BV480		CD337 (Nkp30)	BB700		CD158f (KIR2DL5)	BV421
	CD57	FITC		CD160	PE		CD159a (NKG2A)	BV605
	CD27	APC-R700		CD244 (2B4)	PE-CF594		TIGIT	BV650
CD16	APC-H7	CD314 (NKG2D)	PE-Cy7	CD158a (KIR2DL1)	APC			

Figure 4

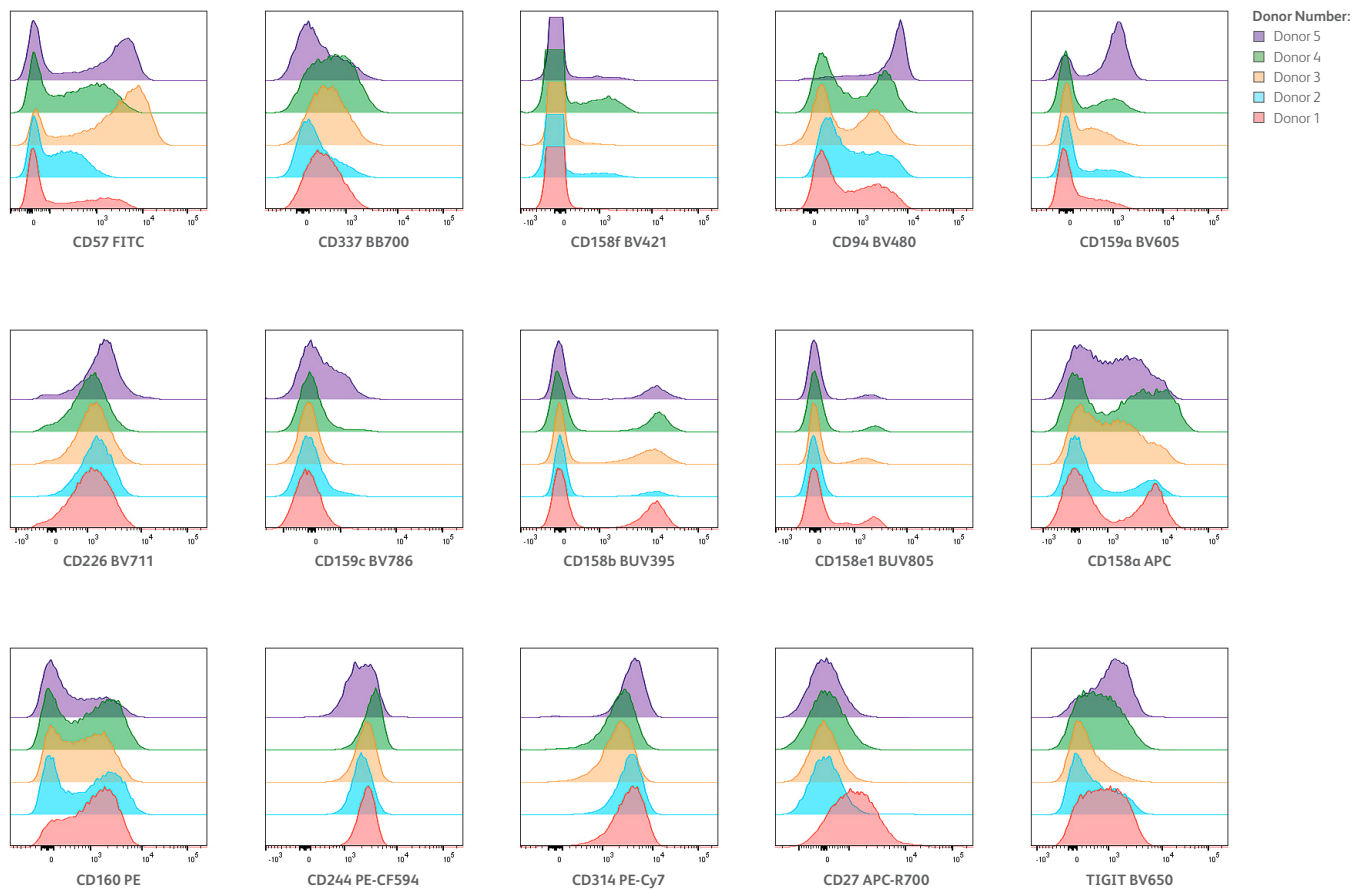


Figure 4. Assessment of stimulatory and inhibitory markers on the surface of NK cells using the 18-color flow cytometry panel

Fresh blood cells from healthy donors were stained as described in Figure 1 with the antibody-fluorochrome conjugates listed in Table 2. Sample acquisition was completed on the BD LSRFortessa X-20 flow cytometer with an ultraviolet/violet/blue/yellow-green/red laser configuration. The expression of stimulatory and inhibitory markers, in addition to CD94, CD57 and CD27, was assessed in CD56<sup>dim</sup>CD16<sup>+</sup> NK cells for different donors, as shown in the histogram layouts. Notable differences in the expression of markers, such as CD57, CD337, CD94, CD159a, CD158a and TIGIT were observed across donors.

For a comprehensive assessment of the NK-cell repertoire, t-Distributed Stochastic Neighbor Embedding (t-SNE) analysis was performed in FlowJo™ software. Use of the t-SNE algorithm enabled simultaneous assessment of independently run samples from different donors (Figure 5A) and simplified donor-to-donor comparison using the heat maps for one marker at a time (Figure 5B). The variable clustering across the donors is driven by the differences in the expression of some of the tested markers such as CD57, CD94 and CD158a. Simplified Presentation of Incredibly Complex Evaluations (SPICE) algorithm was used to identify distinct NK-cell subsets based on selected stimulatory and inhibitory markers (CD94, CD159a {NKG2A}, CD160, CD337, CD158a and CD158b) (Figure 6). Thirty major subsets of NK cells were identified based on combinatorial expression of the selected markers. As indicated in SPICE analysis by the relative sizes of the wedges and layout of arcs, this combinatorial analysis of the stimulatory and inhibitory markers in an 18-color panel reveals intrinsic differences in receptor expression among healthy donors and provides a deeper understanding of the NK-cell diversity.

Figure 5A

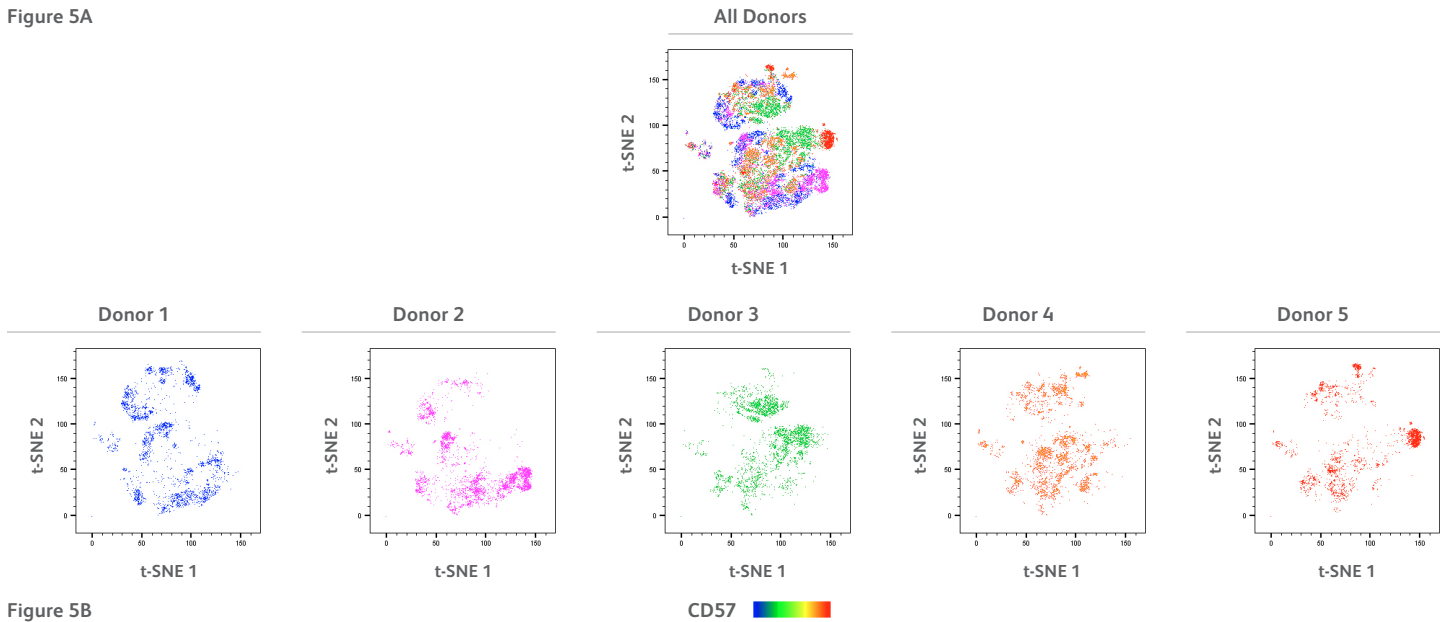


Figure 5B

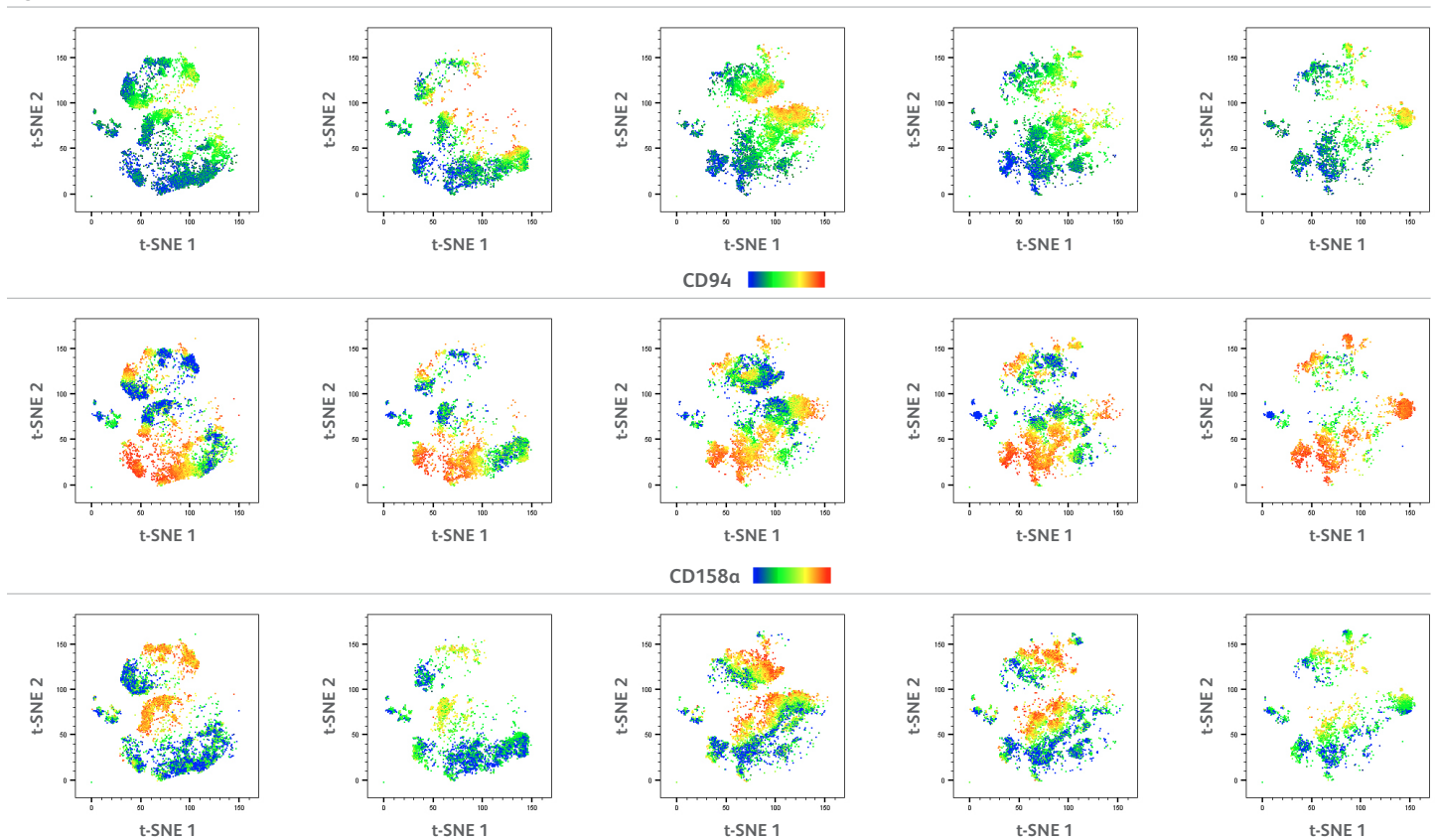
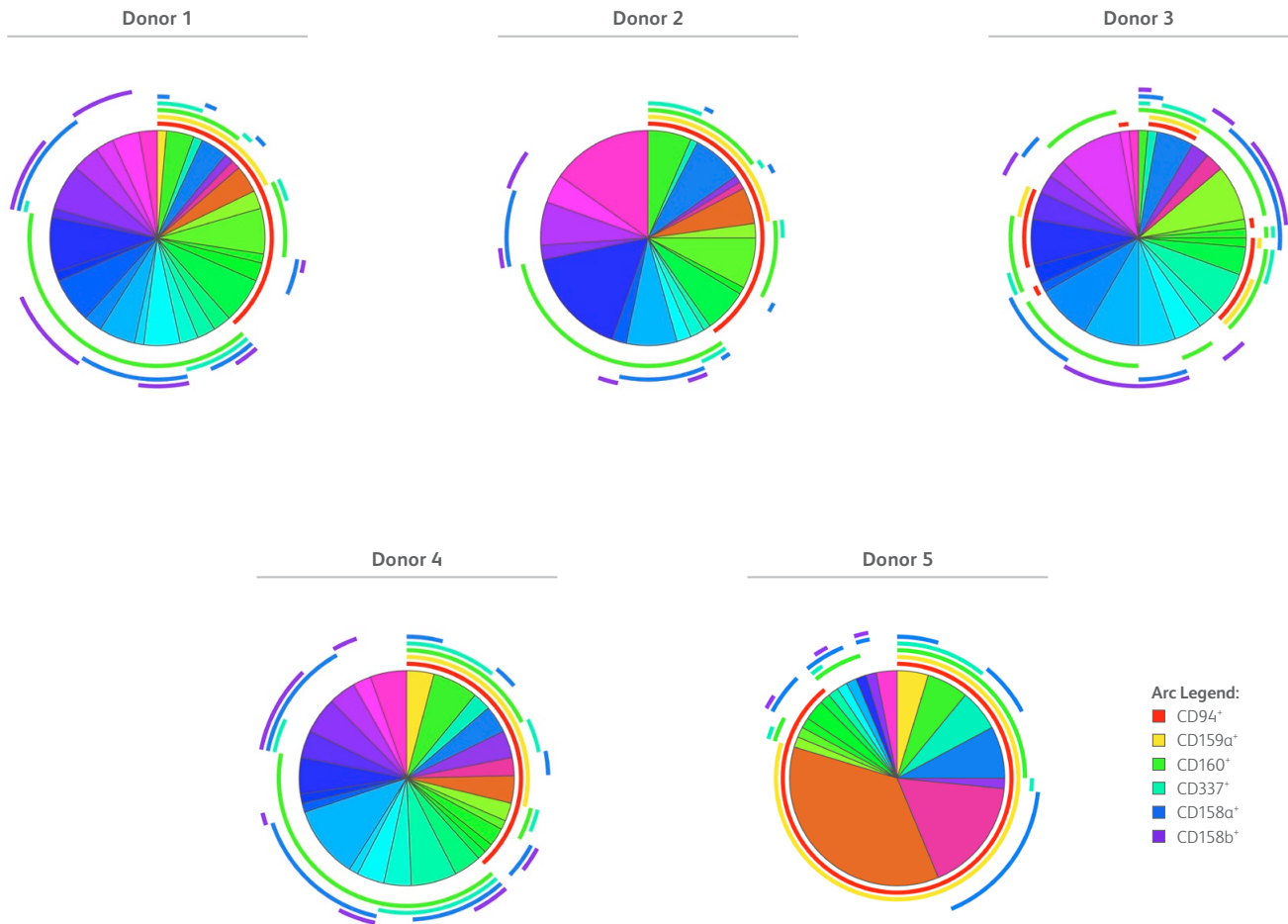


Figure 5. High-dimensional analysis of stimulatory and inhibitory markers on NK cells and comparison of different donors

Fresh blood cells from the five different donors stained and acquired as described in Figure 4 were used for high-dimensional data analysis using FlowJo software. NK cells were gated as CD3<sup>+</sup>CD56<sup>+</sup> for the analysis. **A.** t-SNE analysis for all donors and each individual donor projects donor-to-donor variability in NK-cell stimulatory and inhibitory receptor expression. **B.** Expression of various receptors on the NK-cell surface across different donors, as shown by the heat maps on the donor-specific t-SNE projections. Significant differences in the expression of some of the tested markers (such as CD57, CD94 and CD158a) drive the variable clustering across donors.



Figure 6



**Figure 6. Combinatorial analysis of selected stimulatory and inhibitory receptors across different donors**

Fresh blood cells from different donors (stained and acquired as described in Figure 4) were used for high-dimensional data analysis by the SPICE algorithm. Thirty major subsets of NK cells (pie wedges) were identified based on combinatorial expression of the six markers (arcs) selected: CD94, CD159a (NKG2A), CD160, CD337, CD158a and CD158b. The pie-chart wedges show the relative sizes of the subsets of cells expressing a combination of markers, while the arcs show the expression of selected markers indicated in the arc legend in different subsets, revealing the intrinsic differences in NK-cell repertoire across five healthy donors.

The use of a high-performance instrument along with the proper tools and practices for high-dimensional data analysis provides a robust and efficient approach for comparative and simultaneous combinatorial analysis revealing intrinsic NK-cell diversity among different healthy donors.

The BD LSRFortessa X-20 flow cytometer equipped with the 355-nm UV laser allows the simultaneous analysis of up to 18 markers in a single tube. This is critical to properly characterize cell types with high heterogeneity and phenotypic complexity, such as the NK cells shown in this data sheet. Using this powerful instrument in combination with a series of BD Horizon Brilliant Ultraviolet reagents, provides up to six additional commercially available dyes that are excited by the UV laser and are designed to have minimal overlap with each other. This allows researchers more fluorochrome choices, spread across five spatially separated lasers when designing panels, which can decrease spectral overlap and improve resolution of the specificities of interest. Moreover, when using BD OptiBuild™ custom reagents, the choice of antibody-fluorochrome conjugates greatly expands, enabling easier panel design.

## Ordering information

### Systems and software

#### Description

BD LSRFortessa™ X-20 Cell Analyzer—Special Order

BD LSRFortessa™ Cell Analyzer

### Reagents

Description	Cat. No.
BD FACS™ Lysing Solution 10X Concentrate	349202
BD Pharmingen™ Stain Buffer (FBS)	554656
BD Pharmingen™ FITC Mouse Anti-Human CD57 Clone NK-1	555619
BD Pharmingen™ PE Mouse Anti-Human NKB1 (CD158e1) Clone DX9	555967
BD Pharmingen™ PE-Cy™7 Mouse Anti-Human CD56 Clone B159	557747
BD Pharmingen™ APC-H7 Mouse Anti-Human CD3 Clone SK7	560176
BD Pharmingen™ APC-H7 Mouse Anti-Human CD16 Clone 3G8	560195
BD Pharmingen™ PE Mouse Anti-Human CD160 Clone BY55	562118
BD Pharmingen™ APC Mouse Anti-Human CD244 Clone 2-69	562350
BD Pharmingen™ PE-Cy™7 Mouse Anti-Human CD314 (NKG2D) Clone 1D11	562365
BD Horizon™ BV786 Mouse Anti-Human CD16 Clone 3G8	563690
BD Pharmingen™ APC Mouse Anti-Human CD158a Clone HP-3E4	564319
BD Horizon™ BUV737 Mouse Anti-Human CD56 Clone NCAM16.2	564447
BD Horizon™ BV711 Mouse Anti-Human CD226 Clone DX11	564796
BD Horizon™ PE-CF594 Mouse Anti-Human CD244 Clone 2-69	564881
BD Horizon™ APC-R700 Mouse Anti-Human CD27 Clone M-T271	565116

### Reagents

Description	Cat. No.
BD Horizon™ BV421 Mouse Anti-Human CD158f Clone UP-R1	566330
BD Horizon™ Brilliant Stain Buffer Plus	566385
BD Horizon™ BUV737 Mouse Anti-Human CD56 Clone NCAM16.2	612766
BD OptiBuild™ BUV563 Mouse Anti-Human CD3 Clone SK7	741448
BD OptiBuild™ BV650 Mouse Anti-Human CD337 (NKp30) Clone p30-15	743171
BD OptiBuild™ BV605 Mouse Anti-Human CD158b Clone CH-L	743453
BD OptiBuild™ BUV395 Mouse Anti-Human CD158b Clone CH-L	743456
BD OptiBuild™ BV421 Mouse Anti-Human CD314 (NKG2D) Clone 1D11	743558
BD OptiBuild™ BB700 Mouse Anti-Human CD337 (NKp30) Clone p30-15	745937
BD OptiBuild™ BV786 Mouse Anti-Human CD159c (NKG2C) Clone 134591	748170
BD OptiBuild™ BV480 Mouse Anti-Human CD94 Clone HP-3D9	746737
BD OptiBuild™ BV650 Mouse Anti-Human TIGIT Clone 741182	747840
BD OptiBuild™ BV711 Mouse Anti-Human NKG2A (CD159a) Clone 131411	747919
BD OptiBuild™ BV605 Mouse Anti-Human NKG2A (CD159a) Clone 131411	747921
BD OptiBuild™ BV605 Mouse Anti-Human CD159c (NKG2C) Clone 134591	748166
BD OptiBuild™ BUV805 Mouse Anti-Human CD158e1 (NKB1) Clone DX9	748921

Class 1 Laser Product.

For Research Use Only. Not for use in diagnostic or therapeutic procedures.

Cy™ is a trademark of GE Healthcare.

23-21435-00

BD Life Sciences, San Jose, CA, 95131, USA

[bdbiosciences.com](http://bdbiosciences.com)

BD, the BD Logo, FACS, FlowJo, Horizon, Horizon Brilliant, LSRFortessa, OptiBuild and Pharmingen are trademarks of Becton, Dickinson and Company or its affiliates. All other trademarks are the property of their respective owners. © 2019 BD. All rights reserved.

